Building and Environment 261 (2024) 111716

Contents lists available at ScienceDirect

Building and Environment

journal homepage: www.elsevier.com/locate/buildenv

Functional biocarbon-based coatings for wood protection and indoor air depollution

Mariem Zouari [a,b,*], Laetitia Marrot [c], David B. DeVallance [d]

[a] InnoRenew CoE, Livade 6a, 6310, Izola, Slovenia
[b] Faculty of Mathematics, Natural Sciences, and Information Technologies, University of Primorska, Muzejski Trg 2, 6000, Koper, Slovenia
[c] FRISSBE, Slovenian National Building and Civil Engineering Institute (ZAG), 1000, Ljubljana, Slovenia
[d] College of Science and Technology, Commonwealth University of Pennsylvania, 401 North Fairview Street, Lock Haven, PA, 17745, United States

ARTICLE INFO

Keywords:
Photocatalytic wood coatings
Hydrophobic surface
UV protection
Volatile organic compound
Formaldehyde removal

ABSTRACT

Growing concerns about indoor air pollution heighten the need to develop depolluting materials to achieve a healthy built environment. This study developed functional coatings for wooden surfaces using 20 wt% photocatalytic biocarbon particles doped with manganese oxide (BC–MnO_2) and two different coating materials (linseed oil and waterborne acrylic). The samples' surface hydrophobicity and color properties were tested before and after accelerated aging. The depolluting potential of the samples was evaluated by formaldehyde removal efficiency test in indoor conditions. Results showed that adding BC-MnO_2 particles increased the hydrophobicity regardless of the coating material's type. After accelerated aging, the hydrophobicity of all samples increased, which was attributed to the curing of the oil and acrylic polymers and the increase in surface roughness eventually caused by surface damage. The color change (ΔE) was more intense in the case of uncoated wood and samples without BC-MnO_2. However, the BC-MnO_2-containing coatings were effective in color preservation ($\Delta E < 2$), which was attributed to the *anti*-UV property of biocarbon. The BC-MnO_2-containing coatings exhibited a promising formaldehyde removal efficiency of up to 24 % and 46 % for oil and acrylic samples, respectively. The combination of BC-MnO_2 and acrylic material was more favourable to attracting the formaldehyde molecules, likely due to the similar polarity. The developed functional coatings exhibited an acceptable ability for wood protection and formaldehyde remediation and can be potentially used to enhance indoor air quality.

1. Introduction

Achieving a healthy indoor environment remains challenging due to multiple emission sources, increasing the risk of exposure to airborne toxins. Depending on their formulation and manufacturing processes, products such as wood furniture, paints, and coatings are known as potential sources of the release of volatile organic compounds (VOCs). The presence of VOCs in the built environment reduces the air quality we breathe, negatively impacting human health and well-being. On average, an adult inhales 11,000 L of air daily [1]. Therefore, paying rigorous attention to the quality of indoor air is crucial. One way to maintain a healthy and comfortable built environment is to use innovative and harmless materials in our buildings.

Wood materials used indoors are generally coated to improve long-term performance and durability. However, many of the coating materials used result in the off-gassing of VOCs. For instance, Guo and Murray [2] evaluated the total VOC emission from three different types of furniture polish at room temperature in a test chamber. Results showed that the maximum total VOC emissions were 4.25 mg/m^3, 4.52 mg/m^3, and 584 μg/m^3 for aerosol spray, emulsion, and solvent polishes, respectively. In another example, Stachowiak-Wencek et al. [3] studied the emissions from different lacquer products in ambient conditions. They found that the average total VOCs released from the samples after 24 h ranged between 307 μg/m^3 and 1829 μg/m^3. Moreover, they identified the composition of emitted VOCs and reported the presence of aldehydes, esters, ketones, aliphatic, aromatic hydrocarbons, alcohols, glycols, and terpenes. Many of these compounds can negatively influence human health. Reducing the VOC emissions from coatings can help to control the indoor air pollution. Moreover, adding a depolluting function to the coatings can be even better for enhancing and maintaining the indoor air quality.

Research and development efforts devoted to coating systems have

* Corresponding author. InnoRenew CoE, Livade 6a, 6310, Izola, Slovenia.
E-mail addresses: mariem.zouari@innorenew.eu (M. Zouari), laetitia.marrot@zag.si (L. Marrot), ddevallance@commonwealthu.edu (D.B. DeVallance).

https://doi.org/10.1016/j.buildenv.2024.111716
Received 19 January 2024; Received in revised form 29 April 2024; Accepted 2 June 2024
Available online 3 June 2024

experienced rapid growth. As a result, a new generation of products called functional coatings has emerged. Functional coatings provide novel functions besides their conventional role of protection and decoration. The global functional coatings market grew to 460 million euros in 2022 and is forecasted to increase to 680 million euros by 2030 [4]. Common examples of functional coatings include self-healing, anti-microbial, and depolluting coatings. For instance, VOC adsorbing coatings can have great potential in air purification, given the high interaction of air with the coated surfaces. However, research about depolluting coatings is still minimal. Depolluting coatings are passive removal materials capable of removing pollutants with no additional energy consumption [5,6].

Biocarbon (BC) is a porous carbonaceous material that showed promising potential in VOC removal [7]. Prior research [8] found that BC particles produced from the pyrolysis of *Arundo donax* could adsorb formaldehyde efficiently and be reused up to four times using a regenerative thermal treatment process. While these findings are attractive, innovative means of regenerating carbonaceous materials, including BC, are needed for coating and indoor applications. Using photocatalytic agents is one potential option for extending the lifespan of the adsorbent and ensuring continuous pollutant removal. Few studies explored using carbon-based passive removal materials for VOC mitigation in the built environment. For instance, Krou et al. [9] utilized cement paste containing activated carbon (AC) to remove acetaldehyde and toluene. They found that the material reduced the toluene concentration by 37 % compared to only 5 % for the reference sample without AC. Seo et al. [10] investigated the toluene removal efficiency of gypsum boards mixed with AC. They reported a significant increase in pollutant removal after adding AC to the gypsum. Likewise, Zuraimi et al. [11] studied the efficiency of commercialized AC-based wallpaper and found a toluene removal rate of up to 200 mg/m^2/h. Research on using porous carbon materials within coatings is limited. Jeon et al. [12] investigated the toluene removal efficiency of AC mixed with acrylic polymer applied on different surfaces (glass, gypsum, and mortar). The research results showed that the average efficiency of toluene removal of the AC/acrylic coating was up to 98 % and 96 % when tested in a static laboratory experiment and real building environment, respectively. These results indicated the possibilities of carbonaceous materials as a VOC-reducing substances in indoor environments. However, the saturation of the adsorbent remains a key challenge that limits the use of carbon-based passive removal materials for longer periods.

Our prior research [13] examined the formaldehyde removal efficiency of BC particles doped with variable MnO_2 concentrations (2 %–13 %). The BC doped with 8 % MnO_2 exhibited promising formaldehyde removal efficiency (up to 91 %) and stability in ambient conditions and under the presence of visible light. The synergetic effect between the adsorptive property of BC and the photocatalytic activity of MnO_2 led to high remediation performance. The integrated adsorption-photodegradation technology had the advantage of avoiding the saturation of the BC, which enabled continuous removal of the formaldehyde. Indeed, the adsorbed formaldehyde was degraded by the MnO_2, and the BC pores were regenerated. Prior studies reported successful application of carbonaceous material doped with MnO_2 in formaldehyde remediation [13,14]. However, biocarbon-MnO_2 (BC–MnO_2) particles have not been explored in developing wood coatings for formaldehyde removal. In this study, we aimed to use the previously prepared BC-MnO_2 particles to create a functional coating system for wooden surfaces. The main objectives were (i) to evaluate the suitability of the coatings to protect wood by assessing changes in surface hydrophobicity and color properties of the substrates after exposure to accelerated aging, and (ii) to investigate the formaldehyde removal efficiency of the coatings.

2. Materials and methods

2.1. Materials

Waterborne acrylic and linseed oil (Samson Kamnik d. o.o, Slovenia) were used as materials to prepare the coatings. BC doped with MnO_2 particles (BC–MnO_2) was used as the functional component of the coatings. BC was produced by slow pyrolysis of *Arundo donax* canes at 800 °C for 30 min using a heating rate of 1500 °C/h. The BC's preparation process and detailed characterization can be found in Ref. [8]. BC-MnO_2 particles were prepared using the co-precipitation method reported in Ref. [14]. The ratio BC:MnO_2 was optimized in the laboratory to achieve the highest formaldehyde removal efficiency. The BC-MnO_2 particles were prepared by reaction between 0.411 g of $KMnO_4$, 0.338 g of $MnSO_4$, and 2 g of BC in distilled water at 80 °C for 2 h followed by filtration and drying at 80 °C for 24 h. Details about the preparation and characterization of BC-MnO_2 can be found in Ref. [13]. The BC-MnO_2 had a mean particle size of 17.3 ± 0.6 μm.

Beech (*Fagus sylvatica* L) and oak (*Quercus robur*) substrates with dimensions of 11 cm × 7 cm × 1 cm were used as surfaces for applying the coatings. These two wood species were selected due to their common use in Europe for indoor applications. Formaldehyde solution (37 % w/v) was purchased from Carlo Erba reagents (Dasti group, Val de Reuil, France).

2.2. Preparation of the coatings

The acrylic polymer and linseed oil were mixed separately with 20 wt% of BC-MnO_2 particles. The mixtures were then blended by hand and then ultrasonicated for 1 min to ensure an even dispersion of the particles. The BC-MnO_2 content was optimized in preliminary tests. The aim was to maximize the content of BC-MnO_2 in the coatings' formulation. However, adding BC-MnO_2 content higher than 20 wt% generated a very thick mixture that was hard to handle and apply on a surface. Wood substrates were cut from the same board to ensure surface homogeneity.

The obtained mixtures (Acrylic-BC-MnO_2 and oil-BC-MnO_2) were then applied by brushing on the surface of the substrates. Reference samples of uncoated wood and wood coated with acrylic polymer or linseed oil only (i.e., 0 wt% BC-MnO_2) were also prepared for comparison. Wood coated without BC-MnO_2 was selected as reference in this study instead of uncoated wood given that wood used in building is usually coated for protection and durability purposes. Ten different samples were obtained and are described in Table 1.

Coatings were left to dry for 24 h at ambient conditions, then transferred to a conditioning chamber (Kambič KK-8000 CH-2, Semič, Slovenia) set at 20 °C and 65 % relative humidity for one week to allow complete curing of the coatings. Six replicates were prepared for each sample, resulting in 60 total samples.

2.3. Materials characterization

The viscosity of the coating mixtures with and without BC-MnO_2 was

Table 1
Description of the prepared coatings.

Substrate	Sample coating	Coating material	BC-MnO_2, wt%
Beech	Uncoated	_	0
	Oil	Linseed oil	0
	Acrylic	Acrylic	0
	Oil- BC-MnO_2	Linseed oil	20
	Acrylic-BC-MnO_2	Acrylic	20
Oak	Uncoated	_	0
	Oil	Linseed oil	0
	Acrylic	Acrylic	0
	Oil- BC-MnO_2	Linseed oil	20
	Acrylic-BC-MnO_2	Acrylic	20

measured according to standard [15] using a rotational viscometer (ViscoQC, Anton Paar Quantachrome Instruments, Florida, USA) equipped with a CC12/D18 spindle. Measurements were conducted at a 20%–80 % torque interval and 250 rpm speed. The volume of each tested sample was 11.8 ml per technical manual requirements, and the viscosity was determined at 20 °C and 40 °C. Three repetitions were conducted for each measurement, and average values were reported.

The thickness of BC-MnO_2-containing coatings was determined by microscopic cross-sectional observation using a digital microscope Keyence VHX-6000 (Keyence corporation, Itasca, IL, USA).

The accelerated aging tests were performed by placing samples in an artificial weathering machine (QUV/Spray/RP, QLab corporation, Ohio, USA) equipped with UVA-340 lamps. The coating systems were exposed to an aging cycle by alternating between 16 h of UV exposure (0.68 W/m^2) and 60 °C followed by 8 h in dark conditions at 60 °C. The cycle was designed to mimic the typical indoor day conditions (alternation between light and dark). The aging cycle was repeated seven times, and the total exposure period was 168 h. Three replicates were used to test the surface properties (hydrophobicity and color) before and after exposure to accelerated aging.

The surface hydrophobicity of the coating systems before and after accelerated aging was assessed by measuring the water contact angle (WCA) following the sessile drop method. The WCA was measured using an optical tensiometer (Attention Theta Flex Auto 4 system, Biolin Scientific, Githenburg, Sweden) equipped with a 3D topography module. Tests were performed at ambient conditions using distilled water. Each measurement consisted of five water drops of 4 μL each, and the WCA values were recorded over 10 s after deposition of the drop on the surface. Average values were determined and reported.

The color properties were evaluated on the surface of the coatings before and after accelerated aging using CIELAB L*a*b* system (lightness, red/green, and blue/yellow components). The measurements were conducted using a Spektromaster 565-45 spectrophotometer (Erichsen, Hemer, Germany). The system parameters were set by default after calibration: D65 illuminant, 10° viewing angle, spectral range 400–700 nm; spectral resolution 10 nm; aperture size 11 mm; and fixed geometry of measurement 45°/0°. The color properties and gloss units were measured in three random regions of each sample, and three replicates were evaluated for each sample type. Color change (ΔE) was determined after accelerated aging using Equation (1). ΔE has no unit and is measured on a scale from 0 to 100, where 0 is less color difference, and 100 indicates complete distortion.

$$\Delta E=((\Delta L^*)^2+(\Delta a^*)^2+(\Delta b^*)^2)^{1/2} \quad (1)$$

Where ΔL, Δa, and Δb represent the differences between color coordinate values measured for samples before and after accelerated aging.

2.4. Formaldehyde removal potential of the coatings

The formaldehyde removal potential of the coated samples with and without BC-MnO_2 was evaluated by static experiment adopted from Ref. [12]. Uncoated wood substrates were not considered in the formaldehyde removal test as the objective of the research was to investigate the impact of adding BC-MnO_2 to traditional wood coatings. For each test, a coated substrate was placed in a glass chamber with a volume of 25 L. The uncoated parts of the substrate were covered with aluminum tape to avoid the interaction of the formaldehyde with the uncoated surface. The chamber contained an electrochemical formaldehyde gas sensor (Stox-HCHO, EC Sense, Schäftlarn, Germany) with 0.1 ppm resolution and 1 s response time to detect the changes in formaldehyde concentration. Formaldehyde solution was injected, and the chamber was hermetically closed. The initial formaldehyde concentration in the test chamber stabilized at 4.91 mg/m^3 (equivalent to 4 ppm). The fluctuation of formaldehyde concentrations was tracked continuously for 8 h, noting that the experimental time was selected based on daylight availability. Indeed, previous results showed that the MnO_2 particles were only active and capable to photodegrade the adsorbed formaldehyde under visible light and not under dark conditions [13]. Experiments were performed in ambient indoor conditions: 23 °C, relative humidity 40 %, and conventional visible light. The tests were carried out without a fan in the chamber to avoid disturbing the sensor's stability by intensive air circulation in the small test chamber.

The samples' formaldehyde removal efficiency was determined based on the initial and residual formaldehyde concentrations after 8 h using Equation (2).

$$\text{Formaldehyde removal efficiency } (\%) = \frac{C_i - C_f}{C_i} \times 100 \quad (2)$$

Where C_i is the initial formaldehyde concentration (mg/m^3), and C_f is the final formaldehyde concentration after 8 h of the experiment (mg/m^3).

A blank test was performed by repeating the same experiment without the presence of the sample. The reduction in formaldehyde concentration obtained for the blank was considered when determining the formaldehyde removal potential of the samples. Measurements from three replicates were collected, and average results were reported.

The formaldehyde removal capacity (Q) per coating surface area was determined using Equation (3).

$$Q\ (mg\,/\,m^2) = \frac{(C_i - C_f) \times V}{SA} \quad (3)$$

Where C_i is the initial formaldehyde concentration (mg/L), C_f is the final formaldehyde concentration after 8 h of the experiment (mg/L), V is the volume of the test chamber (L), and SA is the surface area of the coating (m^2).

The sample with the highest formaldehyde removal potential was tested for five repetitive cycles to evaluate its re-usability. At the end of each reuse cycle, a new formaldehyde injection was made without opening the test chamber. The re-emission of the removed formaldehyde was not a concern given that the BC-MnO_2 particles utilized in this study were found to be capable of degrading the adsorbed formaldehyde into less harmful intermediates [13]. Given that formaldehyde can naturally occur in wood, the formaldehyde emissions from the beech and oak substrates were determined to investigate if natural emissions can interfere with the removal test results. Wood substrate was placed in the test chamber without injection of formaldehyde. The emission of formaldehyde was tracked using the same electrochemical sensor.

2.5. Statistical evaluation

The collected data were analyzed for statistically significant differences ($\alpha = 5$ %) using a paired *t*-test in SPSS software (IBM SPSS statistics 26) to evaluate the effect of accelerated aging on WCA and color properties, as well as to compare the formaldehyde removal potential of the coatings on beech and oak.

Table 2
Viscosity values of the coating mixtures with and without BC-MnO_2 particles.

Sample ID	Viscosity, mPa.s	
	20 °C	40 °C
Oil	49.42 ± 1.08	26.62 ± 0.94
Acrylic	125.40 ± 0.75	110.87 ± 7.05
Oil-BC-MnO_2	129.24 ± 2.14	82.37 ± 0.86
Acrylic-BC-MnO_2	1008.05 ± 16.64	662.65 ± 8.21

3. Results and discussion

3.1. Properties of the coatings

The viscosity of the coating mixtures determined at 20 °C and 40 °C are represented in Table 2.

The viscosity of linseed oil at 20 °C (49 mPa s) was similar to the 53 mPa s result reported by Calligaris et al. [16]. The viscosity of acrylic material (125 mPa s) was higher than that of linseed oil. The obtained acrylic viscosity value was slightly lower than previous research [17], where values between 144 and 373 mPa s were reported for waterborne acrylic and latex materials, respectively. The difference between the findings may be attributed to differences in the tested coatings' composition (i.e., solid content, water, etc.). Adding BC-MnO_2 particles increased the viscosity of the linseed oil and the acrylic material by 161 % and 704 %, respectively. This increment was expected because increasing the solid content in the coatings formulations can result in a higher viscosity. The increased viscosity is favourable because it will limit the sedimentation of the particles within the matrix. In this regard, Belgacem et al. [18] reported that the viscosity of linseed oil-based alkyd resins measured at 20 °C increased by around 100 % when organosolv lignin filler particles (20 wt%) were added to the emulsion. Similarly, Scolaro et al. [19] found that the viscosity of resin coatings increased after adding TiO_2 and silver fillers. They indicated that adding fillers facilitated the cross-linking of the resin polymers, which resulted in higher compactness of the matrix. The viscosity values from measurements at 40 °C were lower than those obtained at 20 °C regardless of the sample type. At 40 °C, the linseed oil and acrylic polymers likely started to loosen and increased mobility under the effect of temperature, which decreased the viscosity. Generally, the viscosity of liquids tends to decrease with increasing the temperature due to the increase in kinetic energy of the liquid molecules. The increase in kinetic energy results in reducing the resistance to flow and augmenting the molecules' mobility which is reflected by a decrease in the viscosity. Prior study [20] reported that the viscosity of linseed oil gradually decreased when temperature was increased from 20 °C to 80 °C which was attributed to the expansion and decrease in intermolecular attraction between the oil molecules. In another study, Hamilton and Quail [21]. observed similar trends and reported that the viscosity of lubricant oil decreased as temperature increased from 0 °C to 100 °C. They indicated that increasing the temperature initiated the oxidation and the degradation of the oil components, which lowered the viscosity.

Coatings viscosity plays an important role in both products' appearance and performance. A certain viscosity is necessary for adequate film formation and surface covering. Indeed, a coating with too high viscosity (i.e., very thick) can be hard to handle and may lead to high film thickness, which wastes coating's material and can result in the formation of drip marks [22]. In contrast, a coating with too low viscosity (i.e., very thin) may not achieve the desired film build which will not be satisfactory for surface protection. Therefore, optimizing the materials viscosity when developing coatings is crucial. The selection of coatings' application method is dependent on the materials' rheology. In general, higher viscosity is more favourable for brushing and rolling applications while lower viscosity is better for spraying applications [23]. However, viscosity measurement alone is not fully sufficient to decide the suitable application method [22]. The application method depends on both viscosity and shear rate. For instance, brushing was estimated to generate a shear rate of approximately 10^3-10^6 s^{-1} [24]. Based on this, the estimated viscosity for an effective brushing application is $\leq$ 1000 mPa s approximately [23]. Hence, considering the viscosity measurements obtained for the coating mixtures prepared during this study (Table 2), all samples were suitable for brushing application on the wood substrates.

The thickness of the acrylic-BC-MnO_2 and oil-BC-MnO_2 coatings was 29 ± 7 μm and 27 ± 2 μm on beech and 49 ± 5 μm and 37 ± 7 μm on oak, respectively. The determination of thickness was only possible for the coatings containing BC-MnO_2 particles. However, in the case of reference coatings (without BC-MnO_2), the observation was limited due to the transparent color of the materials.

3.2. Efficiency of the coatings in wood protection

The WCA values on the samples' surface before and after accelerated aging are represented in Table 3.

The uncoated beech exhibited a hydrophilic character, unlike the uncoated oak which had a relatively high WCA (Table 3). Prior research [25] reported similar findings for uncoated beech and oak surfaces (WCA of 56° and 81°, respectively). Tyloses in oak likely contributed to its increased hydrophobicity since tyloses block the liquids' penetration through the vessels.

After coating with linseed oil and acrylic material, the WCA increased for both species. However, linseed oil further improved the surface hydrophobicity compared to the acrylic material. The lower performance of the acrylic material was likely due to its waterborne character. Additionally, linseed oil has been recognized for its capacity as an efficient water-repellent for wood protection. Indeed, as a drying oil, linseed oil can form a protective film on the wood pores and block the lumen, limiting access to water into the internal wood structure [26]. Adding BC-MnO_2 particles to the coatings further enhanced the surface hydrophobicity (Table 3). The WCA of oil coatings after adding BC-MnO_2 increased by 12 % and 9 % for beech and oak, respectively. In the case of acrylic-based coatings, the WCA on beech increased by 13 % after adding BC-MnO_2 particles, while the WCA on oak increased by only 2 %. The increase in surface hydrophobicity after adding BC-MnO_2 particles to the coatings can be attributed to the hydrophobic character of the utilized BC particles. Specifically, the BC particles had a relatively high fixed carbon content (76 %) and aromatic feature (results presented in Ref. [8]), contributing to their hydrophobic nature. Another reason for the increase in WCA can be the effect of BC-MnO_2 particles on the surface topology (i.e., the effect on roughness). Indeed, according to Cassie-Baxter theory, the surface roughness forms air pockets between the liquid drop (i.e., water) and the surface, inhibiting the liquid penetration and increasing the WCA. Amirchand et al. [27] achieved a superhydrophobic surface (i.e., WCA >150°) by coating with non-modified BC particles that were dispersed in ethanol via ultrasonication and applied on a polyurethane tape. They reported that the BC particles on the surface created a super-repellent coating by increasing the roughness and trapping air underneath the water drops.

After the accelerated aging, the WCA of all samples increased regardless of the coating type and wood species (Table 3). Paired *t*-test showed that the increase in WCA after accelerated aging was statistically significant ($P < 0.05$) for uncoated, acrylic, and acrylic-BC-MnO_2 in the case of beech and oak (Table 3). For uncoated beech and oak, the increase in WCA after aging was likely due to changes in wood surface

Table 3
Water contact angle results before and after accelerated aging.

Substrate	Sample	Water contact angle, °		
		Before accelerated aging	After accelerated aging	P-value
Beech	Uncoated	52 ± 4	78 ± 5	<0.001[a]
	Oil	108 ± 1	110 ± 2	0.074
	Acrylic	87 ± 1	94 ± 3	0.026[a]
	Oil-BC-MnO_2	121 ± 13	127 ± 3	0.408
	Acrylic- BC-MnO_2	98 ± 2	107 ± 1	0.004[a]
Oak	Uncoated	93 ± 1	100 ± 2	0.007[a]
	Oil	101 ± 3	105 ± 5	0.074
	Acrylic	95 ± 1	109 ± 5	0.026[a]
	Oil- BC-MnO_2	110 ± 2	111 ± 3	0.225
	Acrylic- BC-MnO_2	97 ± 2	100 ± 1	0.035[a]

[a] Statistically significant difference.

chemistry caused by exposure to UV and temperature. During wood drying or exposure to a relatively high temperature, the water-soluble extractives tend to migrate and concentrate on the surface, which increases the hydrophobicity. Such a trend was reported as a limitation during wood gluing since extractives on the surface act as a barrier against adhesive penetration [28]. Similar findings were reported by Jankowska et al. [29], who investigated surface properties of four wood species after artificial weathering using UV only for 25 h and a combination of UV, temperature (70 °C), and water spraying for 30 h and 120 h. They found that the WCA on the sample's surface increased regardless of the treatment type. They explained that extractives in the wood leached (especially when water was involved in the weathering process) and accumulated on the surface, causing changes in hydrophobicity.

For linseed oil-based coatings (with and without BC-MnO_2), the increase in WCA after aging was likely due to the polymerization and cross-linking reactions provoked by exposure to UV and temperature. Prior research [30] reported that wood treated with linseed oil required a few weeks of drying to allow polymerization and reach a hydrophobic WCA (i.e., WCA >90°), in contrast to tung oil, which polymerized quickly and provided hydrophobicity to the wood surface right after application. Results were explained by the differences in the oils' composition, consisting of a non-conjugated double bond system in linseed oil and a conjugated triene-dominated fatty acid system in tung oil.

In the case of the acrylic-based coatings (with and without BC-MnO_2), the increase in WCA after accelerated aging was likely related to chemical changes in the acrylic polymers. A decrease in the WCA would be expected if the accelerated aging involved water spraying because of the waterborne character of the acrylic material. However, the aging treatment in this study consisted of exposure to UV and temperature only. Izzo et al. [31] investigated the stability of an aqueous emulsion of acrylic copolymers mixed with other additives. The samples were subjected to artificial aging using UV, temperature, or humidity. Results showed that the WCA of all samples increased after the aging treatment using UV and temperature, which was attributed to the decrease in polar groups on the paints' surfaces. They also suspected that part of the waxy fraction in the coating likely migrated to the surface, increasing the WCA.

In the case of all samples, the increase in WCA after aging can also be associated with the eventual increase in surface roughness. The exposure to aggressive UV conditions and temperature likely initiated the damage on the wood and coatings surface, making it rougher. Jankowska et al. [29] reported that the increase in surface roughness after exposure to UV and water spray occurred due to cracking and surface oxidation.

Overall, the addition of BC-MnO_2 positively impacted the hydrophobicity of the samples for both coating materials, and the samples containing linseed oil and BC-MnO_2 particles had the best water resistance on both beech and oak.

Images of the samples before and after exposure to accelerated aging are represented in Fig. 1. Visual evaluation of the samples' surface indicated that the original color of the uncoated substrates and substrates coated without BC-MnO_2 was changed. However, the color change was not visible for substrates coated with BC-MnO_2. The

Fig. 1. Images of (a) beech and (b) oak substrates before (pictures on top) and after (pictures on bottom) accelerated aging.

alteration of color was more visible in the case of beech (Fig. 1 a) than in oak (Fig. 1 b).

The color change of wood is a common sign of its alteration by the effect of light that induces chemical modifications on the surface, mainly lignin depolymerization. Changes in color properties of the uncoated and coated surfaces after exposure to UV irradiation at 60 °C during accelerated aging are summarized in Table 4.

Results from the statistical comparison between the different color parameters before and after accelerated aging using paired t-tests are represented in Table 5. Values from beech and oak samples were compared separately. The difference between the compared values was considered statistically significant if $P \leq 0.05$.

The coatings containing BC-MnO_2 particles had the lowest L* (Table 4) among all other samples, attributed to the black color of the BC-MnO_2 particles. In the case of uncoated substrates and substrates coated without BC-MnO_2, the change in L* after aging was significant for beech compared to oak (Table 5). The effect of accelerated aging on beech L* was more visible because beech has a naturally lighter color than oak. However, when BC-MnO_2 particles were added to the coatings, the change in L* was less intense for both species (Table 4). Thus, adding BC-MnO_2 particles provided more UV resistance to the wood surface.

Values of a* (green/red color indicator) and b* (blue/yellow color indicator) increased after the accelerated aging for uncoated samples and samples coated with oil and acrylic only (Table 4). The increase in a* and b* indicated an increase in the degrees of redness and yellowness. In the case of coatings containing BC-MnO_2, a* and b* values changed slightly after accelerated aging. In addition, the a* and b* values of BC-MnO_2-containing samples were close to 0 (Table 4), indicating that these samples tended to have a color closer to green and blue shades. Prior research [25] reported that tung oil coatings loaded with BC particles (5, 10, and 20 wt%) had higher greenness and blueness than the reference samples. The changes in a* and b* values followed a similar trend as L* and were more intense in the case of uncoated beech and beech coated without BC-MnO_2 compared to oak. The darker color of oak was likely advantageous in preserving the surface's optical properties. Thus, the intensity of changes in surface color depended on the wood substrate's original optical properties. The greater surface alteration of beech was also confirmed by the color change (ΔE) results (Table 4). Indeed, for uncoated beech and beech coated without BC-MnO_2, ΔE ranged between 16 and 23. A ΔE higher than 12 is usually an indication of a complete change in the color, according to Cui et al. [32]. In the case of uncoated oak and oak coated without BC-MnO_2, ΔE values ranged between 6 and 10, which indicates a visible color alteration ($6 < \Delta E > 12$) [32].

Coating the surface with linseed oil decreased the ΔE by 20 % and 36 % in the case of beech and oak, respectively, compared to the uncoated references. Temiz et al. [33] examined the efficiency of different treatments (chromated copper arsenate, metal-free propiconazole treatment, chitosan, furfuryl alcohol, linseed oil, and tall oil) in the protection of pine wood against artificial weathering. They reported that linseed oil was the most effective in minimizing the color change during 800 h of exposure to artificial weathering conditions among all other samples. However, coating with the acrylic material was not beneficial in reducing the color alteration during the exposure to UV and temperature, as the obtained ΔE values were comparable to the uncoated reference (Table 4). The low performance of the waterborne acrylic can be attributed to its transparent feature, which did not provide enough protection to the surface against UV irradiation. Similarly, prior research [34] reported that the ΔE of wood coated with transparent acrylic paint was similar to that of uncoated wood after 200 h of accelerated aging. They explained that the acrylic paint was transparent, which enabled UV light transmission to the wood surface underneath the coating and led to photo-degradation.

For coatings loaded with BC-MnO_2 particles, ΔE values were < 2, signifying a slight change of color regardless of the wood species and coating material type (i.e., acrylic or linseed oil). Adding BC-MnO_2 particles to the coatings sharply decreases the extent of color change during accelerated aging. Therefore, BC-MnO_2-containing coatings were highly effective in preserving the wood surface and avoiding alteration. These findings were attributed to the coatings' black pigmentation,

Table 5
Paired *t*-test results.

Sample type	P-values			
	L*	a*	b*	Gloss
Beech	0.001[a]	0.001[a]	0.001[a]	0.070
Oak	0.464	0.004[a]	0.001[a]	0.505

[a] Statistically significant difference.

Table 4
Color properties before and after accelerated aging.

Substrate	Sample	Color parameters								
		Before accelerated aging				After accelerated aging				Color change (ΔE)[a]
		L*	a*	b*	Gloss	L*	a*	b*	Gloss	
Beech	Uncoated	75.29 ± 0.33	8.26 ± 0.12	20.58 ± 0.01	3.08 ± 0.11	62.38 ± 0.09	15.9 ± 0.07	34.35 ± 0.07	2.67 ± 0.09	20.42
	Oil	70.72 ± 0.43	10.1 ± 0.25	23.96 ± 0.37	2.90 ± 0.08	60.28 ± 0.29	16.42 ± 0.12	34.82 ± 0.74	2.75 ± 0.21	16.33
	Acrylic	75.53 ± 0.36	7.74 ± 0.25	23.82 ± 0.16	14.33 ± 1.02	63.66 ± 0.08	16.12 ± 0.06	41.48 ± 0.14	9.80 ± 1.78	22.87
	Oil-BC-MnO_2	20.59 ± 0.19	0.26 ± 0.01	0.42 ± 0.01	0.51 ± 0.02	22.15 ± 0.19	0.16 ± 0.01	0.58 ± 0.03	0.37 ± 0.03	1.56
	Acrylic- BC-MnO_2	21.48 ± 0.26	0.44 ± 0.01	0.23 ± 0.01	1.31 ± 0.11	21.44 ± 0.08	0.22 ± 0.02	0.29 ± 0.07	0.86 ± 0.39	0.23
Oak	Uncoated	60.12 ± 0.82	8.35 ± 0.23	21.11 ± 0.30	2.91 ± 0.31	57.9 ± 0.34	10.93 ± 0.14	30.71 ± 0.52	2.64 ± 0.49	10.18
	Oil	51.59 ± 0.24	12.47 ± 0.25	28.09 ± 0.44	3.70 ± 0.19	52.29 ± 0.30	13.98 ± 0.10	34.35 ± 0.64	3.19 ± 0.4	6.47
	Acrylic	54.28 ± 0.29	9.96 ± 0.16	29.96 ± 0.39	26.22 ± 2.98	52.34 ± 0.65	12.89 ± 0.13	39.46 ± 0.10	22.41 ± 3.53	10.12
	Oil- BC-MnO_2	22.5 ± 0.30	0.22 ± 0.03	0.27 ± 0.02	1.47 ± 0.12	24.09 ± 0.22	−0.01 ± 0.02	0.32 ± 0.02	1.35 ± 0.18	1.60
	Acrylic- BC-MnO_2	22.62 ± 0.14	0.46 ± 0.05	0.51 ± 0.05	1.74 ± 0.05	22.87 ± 0.04	0.11 ± 0.02	0.78 ± 0.04	0.93 ± 0.04	0.51

L* indicates lightness, a* indicates green/red color, and b* indicates blue/yellow color.
[a] ΔE values were determined using average values from L*, a*, and b*, thus, no standard deviations were reported.

which helped prevent the UV irradiation from passing to the lignin polymers on the surface and initiating their depolymerization. The efficiency of black coatings in preserving wood color was previously reported. For instance, Marrot et al. [25] reported that wood coated with BC-tung oil had a smaller color change after six months of natural weathering than wood coated with tung oil. Results were attributed to the ability of BC to act as a UV absorber, which improved the photostability of the wood surface. In another example, Poohphajai et al. [35] observed a negligible change in the color of wood protected by black fungi bio-finish after a whole year of outdoor weathering. They explained that the black pigment (i.e., melanin) produced by the fungi served as a protective layer against environmental factors that could initiate wood degradation, including protection against light and UV irradiation.

Changes in surface glossiness are also an indicator of wood degradation. The change in glossiness after accelerated aging was not statistically significant (Table 5) in the case of all samples. These findings were different compared to findings from other studies. For instance, it was reported that exposure to artificial [36] or natural [25] weathering was correlated with a decrease in the glossiness of wood surfaces. However, in the reported studies, water spray or rain factors were involved in the aging process, likely contributing to decreased glossiness. Further investigation of gloss value behaviors over a more extended period of accelerated aging might be necessary to make proper conclusions regarding this point.

3.3. Efficiency of the coatings in formaldehyde remediation

The measured formaldehyde emissions from beech and oak substrates are provided in Fig. A1 (Appendix A). The natural formaldehyde emissions from the uncoated wood substrates were less than 0.01 ppm regardless of the wood species. Formaldehyde emissions from the used substrates were negligible and not a concern in this study. Böhm et al. [37] evaluated the formaldehyde emissions from different wood species according to EN 717-1 standard. They found that formaldehyde emissions from beech and oak were 0.0068 ± 0.001 ppm and 0.0042 ± 0.0003 ppm, respectively, which seems to be relatively low. In general, formaldehyde, occurring naturally in wood, is primarily off-gassed during the drying phase. In contrast, wood-based composites are recognized as the primary emission source of formaldehyde indoors [38]. These emissions are mainly associated with the use of synthetic adhesive (e.g., urea-formaldehyde) in commercial particle boards and furniture.

Table 6 represents the formaldehyde removal efficiency and capacity of the coatings with and without BC-MnO_2 particles determined after 8 h in ambient conditions.

A paired *t*-test showed a statistically significant difference between the formaldehyde removal potential of the coatings on beech and oak ($P = 0.021$). Regardless of the substrate type, coatings without BC-MnO_2 exhibited a relatively low formaldehyde removal efficiency of approximately 3 % and 6 % for linseed oil and acrylic, respectively. The formaldehyde removal in the case of samples without BC-MnO_2 was attributed to the adsorption of pollutant molecules on the surface of the coatings. Despite the absence of porous adsorbent material in the samples, some formaldehyde molecules likely interacted with the surface (linseed oil and acrylic). However, this part was relatively low. The formaldehyde removal increased after adding BC-MnO_2 particles to the coatings (Table 6). The removal efficiency of the linseed oil-based coatings increased by 700 % and 476 % on beech and oak, respectively. Likewise, the removal efficiency of the acrylic-based coatings increased by approximately 650 % on both beech and oak after adding BC-MnO_2. The variation of formaldehyde concentrations in the test chamber (Fig. A 2 and Fig. A 3 in Appendix A) showed that the decrease in formaldehyde concentration was faster in the case of coatings containing BC-MnO_2 compared to the reference sample. Moreover, the formaldehyde removal rate was faster in the case of acrylic-BC-MnO_2 coatings compared to the oil-BC-MnO_2 ones. The formaldehyde removal potential of the coatings was attributed to the integrated adsorption-photocatalytic degradation activity of the BC-MnO_2 particles. The utilized BC has a relatively high adsorptive potential due to its well-developed microporous structure. The microporous surface area of the utilized BC is 587.18 m^2/g, which enabled the capture of the formaldehyde molecules via a pore-filling mechanism [8]. Moreover, the MnO_2, a visible light photocatalyst, degraded the captured formaldehyde, resulting in the regeneration of the BC pores and making them available for further adsorption. The synergetic effect between carbonaceous materials and MnO_2 particles for removing formaldehyde was previously confirmed. For instance, Zhang et al. [39] used MnO_2 loaded on activated carbon paper to remove formaldehyde in ambient conditions and achieved 59 ppm of formaldehyde reduction in 10 h.

Regardless of the wood substrate, the acrylic-BC-MnO_2 coatings performed twice better than the oil-BC-MnO_2 coatings (Table 6). This difference in formaldehyde removal was likely caused by the difference in polarity of the linseed oil and the acrylic material, which influenced the interaction of the coating with the formaldehyde molecules. Formaldehyde, as a polar compound, had likely higher affinity to the polar acrylic surface, while the apolar oil surface was less favourable for interaction. This assumption can be supported by the surface hydrophobicity results (Table 3), which revealed that linseed oil-coated substrates were more hydrophobic (i.e., apolar) than acrylic-coated samples. Surfaces with higher hydrophobicity are advantageous in the case of adsorption of apolar molecules [40], unlike formaldehyde. Prior research [41] reported that increasing the polarity of activated carbon via oxidation (i.e., incorporation of oxygen functional groups) contributed to increasing the affinity to formaldehyde as a polar molecule. However, the same treatment was not favourable for benzene, a non-polar compound.

The highest formaldehyde removal capacities, 9.3 and 8.5 mg/m^2 achieved by the acrylic-BC-MnO_2 coatings on beech and oak, respectively, can be considered satisfactory for mitigating indoor formaldehyde levels. However, the lifespan of the depolluting coating is important to optimize the possibility of effective use over a long period. The re-useability of the acrylic-BC-MnO_2 sample on beech was evaluated, and its formaldehyde removal efficiency was determined over five successive reuse cycles, as shown in Fig. 2.

The acrylic-BC-MnO_2 coating exhibited a relatively stable performance in removing formaldehyde up to the fourth cycle. At cycle 5, the formaldehyde removal efficiency of the coating decreased by 16 % compared to the fresh sample. The decrease in the coating's performance over reuse cycles can be related to the partial deactivation of the photocatalyst (MnO_2) due to the accumulation of formaldehyde degradation intermediates. Another reason can be the eventual fluctuation of experimental conditions (temperature, relative humidity, and light intensity), given that the experiments were conducted in ambient conditions. Further research will be implemented to investigate the effect of external conditions on the coating's depolluting potential and improve the material's remediation capacity.

Table 6
Formaldehyde removal test results.

Substrate	Sample	Removal efficiency, %	Removal capacity, mg/m^2
Beech	Oil	3.0 ± 0.3	0.6 ± 0.1
	Acrylic	6.2 ± 1.6	1.23 ± 0.3
	Oil-BC-MnO_2	24.2 ± 3.0	4.83 ± 0.6
	Acrylic-BC-MnO_2	46.6 ± 5.1	9.29 ± 1.0
Oak	Oil	3.4 ± 0.2	0.68 ± 0.4
	Acrylic	5.7 ± 1.1	1.14 ± 0.2
	Oil-BC-MnO_2	19.6 ± 3.7	3.91 ± 0.7
	Acrylic-BC-MnO_2	42.6 ± 8.9	8.5 ± 1.8

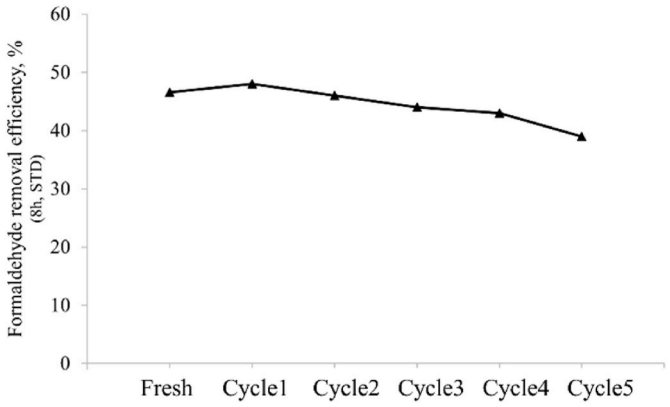

Fig. 2. Formaldehyde removal efficiency of acrylic-BC-MnO_2 coating on beech after five reuse cycles.

4. Conclusion

Enhancing indoor air quality requires optimized and effective strategies. Depolluting materials are convenient solutions that help maintain healthy indoor air quality without additional energy demands. Functional coatings were successfully prepared using two materials (linseed oil and waterborne acrylic) loaded with 20 wt% active BC-MnO_2 particles. The coatings were applied on beech and oak substrates and evaluated for their capacity to protect the wood and to remove formaldehyde in indoor conditions. Surface hydrophobicity of the coatings containing BC-MnO_2 particles was higher compared to the reference samples and ranged from 98° to 121° and from 97° to 110° for beech and oak, respectively. After accelerated aging, the surface hydrophobicity of all samples increased, which was attributed to the increase in surface chemistry and roughness. Regarding color properties, adding BC-MnO_2 particles improved color stability against accelerated aging. It was found that the color change for samples without BC-MnO_2 ranged from 16 to 23 and from 6 to 10 in the case of beech and oak, respectively. However, for samples containing BC-MnO_2, the color change was under 2, attributed to BC's ability to increase photostability against UV irradiation. The coating prepared from acrylic and BC-MnO_2 particles exhibited the highest formaldehyde removal efficiency (46 %) among all samples. Moreover, this coating showed acceptable stability over five reuse cycles. The coatings' depolluting ability was attributed to BC's efficiency as a porous adsorbent and the photocatalytic activity of MnO_2 that enabled formaldehyde degradation. Overall, the acrylic-BC-MnO_2 sample was the best in terms of wood protection and depolluting potential. Functional coatings can be a promising way to mitigate airborne pollutants from the indoor environment due to the large area of coated surfaces in buildings. Further research should be implemented to investigate the performance of these coatings at a larger scale within a building to verify their efficiency in removing VOCs and other polluting compounds.

CRediT authorship contribution statement

Mariem Zouari: Writing – original draft, Methodology, Investigation, Formal analysis, Conceptualization. **Laetitia Marrot:** Writing – review & editing, Conceptualization. **David B. DeVallance:** Writing – review & editing, Supervision, Conceptualization.

Declaration of competing interest

The authors declare that they have no known competing financial interests or personal relationships that could have appeared to influence the work reported in this paper.

Data availability

Data will be made available on request.

Acknowledgments

The authors gratefully thank and acknowledge the funding from the Slovenian Research and Innovation Agency (ARIS) for the projects N2-0225 and J4-4546. Furthermore, the authors thank the Slovenian Ministry of Higher Education, Research, and Innovation for funding the ForestValue Research Programme, specifically the project Bark-Build—tree bark as a renewable source of wood protection materials for building applications [C3330-21-252003]. The authors also acknowledge the support of the European Union's Horizon 2020 research and innovation program under H2020-WIDESPREAD-2018-2020-6 [952395] and investment from the Republic of Slovenia and the European Regional Development Fund.

Appendix A. Supplementary data

Supplementary data to this article can be found online at https://doi.org/10.1016/j.buildenv.2024.111716.

References

[1] Lung care foundation, « lung basics », lung care foundation, Consulté le: 27 avril (2024) [En ligne]. Disponible sur: https://lcf.org.in/lung-basics/.
[2] H. Guo, , et al.F. Murray, Determination of total volatile organic compound emissions from furniture polishes, Clean Prod. Process. 3 (1) (2001) 42–48, https://doi.org/10.1007/s100980100099, juin.
[3] A. Wencek, M. Zborowska, W. Pradzynski, , et al.B. Waliszewska, Emissions of volatile organic compounds from lacquer coatings used in the furniture industry, modified with nanoparticles of inorganic metal compounds, Turk. J. Agric. For. 39 (2) (2015) 251–259, https://doi.org/10.3906/tar-1405-24, janv.
[4] Skyquest, Functional coatings market size, share, growth analysis, by product type, end-user - industry forecast 2022-2028 », Global, SQMIG15E2111 (mars 2023). Consulté le: 22 octobre 2023. [En ligne]. Disponible sur, https://www.skyquestt.com/report/functional-coatings-market.
[5] E.T. Gall, R.L. Corsi, , et al.J.A. Siegel, Barriers and opportunities for passive removal of indoor ozone, Atmos. Environ. 45 (19) (2011) 3338–3341, https://doi.org/10.1016/j.atmosenv.2011.03.032, juin.
[6] D.A. Kunkel, E.T. Gall, J.A. Siegel, A. Novoselac, G.C. Morrison, , et al.R.L. Corsi, Passive reduction of human exposure to indoor ozone, Build. Environ. 45 (2) (févr. 2010) 445–452, https://doi.org/10.1016/j.buildenv.2009.06.024.
[7] X. Zhang, et al., Biochar for volatile organic compound (VOC) removal: sorption performance and governing mechanisms, Bioresour. Technol. 245 (déc. 2017) 606–614, https://doi.org/10.1016/j.biortech.2017.09.025.
[8] M. Zouari, L. Marrot, , et al.D.B. DeVallance, Evaluation of properties and formaldehyde removal efficiency of biocarbon prepared at variable pyrolytic temperatures, Front. Environ. Sci. 11 (2023), https://doi.org/10.3389/fenvs.2023.1252926.
[9] N.J. Krou, et al., Reactivity of volatile organic compounds with hydrated cement paste containing activated carbon, Build. Environ. 87 (mai 2015) 102–107, https://doi.org/10.1016/j.buildenv.2015.01.025.
[10] J. Seo, S. Kato, Y. Ataka, , et al.S. Chino, Performance test for evaluating the reduction of VOCs in rooms and evaluating the lifetime of sorptive building materials, Build. Environ. 44 (1) (janv. 2009) 207–215, https://doi.org/10.1016/j.buildenv.2008.02.013.
[11] M.S. Zuraimi, et al., Performance of sorption- and photocatalytic oxidation-based indoor passive panel technologies, Build. Environ. 135 (mai 2018) 85–93, https://doi.org/10.1016/j.buildenv.2018.03.004.
[12] J. Jeon, J.H. Park, S. Wi, B.Y. Yun, T. Kim, , et al.S. Kim, Field study on the improvement of indoor air quality with toluene adsorption finishing materials in an urban residential apartment, Environ. Pollut. 261 (2020) 114137, https://doi.org/10.1016/j.envpol.2020.114137 juin.
[13] M. Zouari, S. Hribernik, L. Marrot, M. Tzolov, , et al.D.B. DeVallance, « Manganese dioxide-coated biocarbon for integrated adsorption-photocatalytic degradation of formaldehyde in indoor conditions, Heliyon 10 (9) (2024) e29993, https://doi.org/10.1016/j.heliyon.2024.e29993 mai.
[14] Z. Dai, et al., Nanocrystalline MnO2 on an activated carbon fiber for catalytic formaldehyde removal, RSC Adv. 6 (99) (oct. 2016) 97022–97029, https://doi.org/10.1039/C6RA15463H.
[15] ASTM D7867-13, Standard Test Methods for Measurement of the Rotational Viscosity of Paints, Inks and Related Liquid Materials as a Function of Temperature, 2020, https://doi.org/10.1520/D7867-13R20.
[16] S. Calligaris, G. Mirolo, S. Da Pieve, G. Arrighetti, , et al.M.C. Nicoli, Effect of oil type on formation, structure and thermal properties of γ-oryzanol and β-sitosterol-

Based organogels, Food Biophys. 9 (1) (2014) 69–75, https://doi.org/10.1007/s11483-013-9318-z, mars.
[17] K. Ito, T. Kato, , et al.T. Ona, Rapid viscosity determination of waterborne automotive paint emulsion system by FT-Raman spectroscopy, Vib. Spectrosc. 35 (1) (2004) 159–163, https://doi.org/10.1016/j.vibspec.2003.12.017, juin.
[18] M.N. Belgacem, A. Blayo, , et al.A. Gandini, Organosolv lignin as a filler in inks, varnishes and paints, Ind. Crops Prod. 18 (2) (sept. 2003) 145–153, https://doi.org/10.1016/S0926-6690(03)00042-6.
[19] C. Scolaro, L.F. Liotta, C. Calabrese, G. Marcì, , et al.A. Visco, « adhesive and rheological features of ecofriendly coatings with antifouling properties, Polymers 15 (11) (2023), https://doi.org/10.3390/polym15112456.
[20] M. Khan, , et al.S. Hasan, Effects of diesel addition on viscosity of linseed oil and consequent effects on performance characteristics of CI engine. présenté à National Conference on Recent Developments and Future Trends in Mechanical Engineering (RDFTME-2006), Hamirpur, india: NIT Hamirpur, nov. 2006, p. 5.
[21] A. Hamilton, , et al.F. Quail, Detailed State of the Art Review for the Different On-Line/In-Line Oil Analysis Techniques in Context of Wind Turbine Gearboxes, vol. 133, 2011, https://doi.org/10.1115/GT2011-46860.
[22] R.R. Eley, Applied rheology and architectural coating performance, J. Coating Technol. Res. 16 (2) (2019) 263–305, https://doi.org/10.1007/s11998-019-00187-5, mars.
[23] P. Kalenda, Application of associative thickeners to water-borne coatings, Pigment Resin Technol. 31 (oct. 2002) 284–289, https://doi.org/10.1108/03699420210442310.
[24] A.R. Marrion, The Chemistry and Physics of Coatings, Royal Society of Chemistry, 2007.
[25] L. Marrot, M. Zouari, M. Schwarzkopf, , et al.D.B. DeVallance, Sustainable biocarbon/tung oil coatings with hydrophobic and UV-shielding properties for outdoor wood substrates, Prog. Org. Coating 177 (2023) 107428, https://doi.org/10.1016/j.porgcoat.2023.107428 avr.
[26] T. Ulvcrona, H. Lindberg, , et al.U. Bergsten, Impregnation of Norway spruce (Picea abies L. Karst.) wood by hydrophobic oil and dispersion patterns in different tissues, For. Int. J. For. Res. 79 (1) (2006) 123–134, https://doi.org/10.1093/forestry/cpi064, janv.
[27] K.D. Amirchand, K. Kaur, , et al.V. Singh, Biochar based self cleaning superhydrophobic surface with aqueous DESphobic properties, J. Mol. Liq. 380 (2023) 121736, https://doi.org/10.1016/j.molliq.2023.121736 juin.
[28] R.N. Kumar, , et al.A. Pizzi, Wood surface inactivation due to extractives, in: Adhesives for Wood and Lignocellulosic Materials, 1re éd., John Wiley & Sons, Ltd, 2019, pp. 211–222, https://doi.org/10.1002/9781119605584.ch9.
[29] A. Jankowska, K. Rybak, M. Nowacka, , et al.P. Boruszewski, Insight of weathering processes based on monitoring surface characteristic of tropical wood species, Coatings 10 (9) (9, sept. 2020), https://doi.org/10.3390/coatings10090877.
[30] B. Arminger, J. Jaxel, M. Bacher, W. Gindl-Altmutter, , et al.C. Hansmann, On the drying behavior of natural oils used for solid wood finishing, Prog. Org. Coating 148 (nov. 2020) 105831, https://doi.org/10.1016/j.porgcoat.2020.105831.
[31] F.C. Izzo, E. Balliana, E. Perra, , et al.E. Zendri, Accelerated ageing procedures to assess the stability of an unconventional acrylic-wax polymeric emulsion for contemporary art, Polymers 12 (9) (9, sept. 2020), https://doi.org/10.3390/polym12091925.
[32] W. Cui, D.P. Kamdem, , et al.T. Rypstra, Diffuse reflectance infrared fourier transform spectroscopy (drift) and color changes of artificial weathered wood, Wood Fiber Sci. 36 (2004) 291–301.
[33] A. Temiz, N. Terziev, M. Eikenes, , et al.J. Hafren, Effect of accelerated weathering on surface chemistry of modified wood, Appl. Surf. Sci. 253 (12) (avr. 2007) 5355–5362, https://doi.org/10.1016/j.apsusc.2006.12.005.
[34] M. Deka, , et al.M. Petrič, Photo-degradation of water borne acrylic coated modified and non-modified wood during artificial light exposure, Bioresources 3 (2) (févr. 2008) 346–362, https://doi.org/10.15376/biores.3.2.346-362.
[35] F. Poohphajai, J. Sandak, M. Sailer, L. Rautkari, T. Belt, , et al.A. Sandak, Bioinspired living coating system in service: evaluation of the wood protected with biofinish during one-year natural weathering, Coatings 11 (6) (6, juin 2021), https://doi.org/10.3390/coatings11060701.
[36] Ü. Ayata, B. Esteves, L. Gürleyen, N. Çakicier, J. Ferreira, , et al.I. Domingos, This work is licensed under the creative commons attribution 4.0 international license, in: EFFECT of ACCELERATED AGEING on SOME SURFACE PROPERTIES of UV-COATED HACKBERRY (Celtis Australis L.) WOOD PARQUET, vol. 64, janv. 2022, https://doi.org/10.12841/wood.1644-3985.383.09. http://creativecommons.org/licenses/by/4.0.
[37] M. Böhm, M.Z.M. Salem, et al., Srba, « Formaldehyde emission monitoring from a variety of solid wood, plywood, blockboard and flooring products manufactured for building and furnishing materials, J. Hazard Mater. 221 (222) (juin 2012) 68–79, https://doi.org/10.1016/j.jhazmat.2012.04.013.
[38] T. Salthammer, S. Mentese, , et al.R. Marutzky, Formaldehyde in the indoor environment, Chem. Rev. 110 (4) (2010) 2536–2572, https://doi.org/10.1021/cr800399g, avr.
[39] X. Zhang, et al., Preparation of lignocellulose-based activated carbon paper as a manganese dioxide carrier for adsorption and in-situ catalytic degradation of formaldehyde, Front. Chem. 7 (2019). Consulté le: 5 mai 2023. [En ligne]. Disponible sur: https://www.frontiersin.org/articles/10.3389/fchem.2019.00808.
[40] H.-B. Liu, B. Yang, , et al.N.-D. Xue, Enhanced adsorption of benzene vapor on granular activated carbon under humid conditions due to shifts in hydrophobicity and total micropore volume, J. Hazard Mater. 318 (nov. 2016) 425–432, https://doi.org/10.1016/j.jhazmat.2016.07.026.
[41] Z. Yang, et al., Study on coconut shell activated carbon temperature swing adsorption of benzene and formaldehyde, J. Renew. Mater. 10 (12) (2022) 3573–3585, https://doi.org/10.32604/jrm.2022.022031.